ARTICLES

Electron Transfer in Self-Assembled Orthogonal Structures

Anthony Harriman,*,† James P. Rostron,† Michèle Cesario,‡ Gilles Ulrich,§ and Raymond Ziessel*,§

Molecular Photonics Laboratory, School of Natural Sciences, Bedson Building, University of Newcastle, Newcastle upon Tyne, NE1 7RU, United Kingdom, Institut de Chimie des Substances Naturelles, CNRS, F-91128 Gif-sur-Yvette, France, and Laboratoire de Chimie Moléculaire, Ecole Européenne de Chimie, Polymères et Matériaux, Université Louis Pasteur, 25 rue Becquerel, 67087 Strasbourg Cedex 02, France

Received: September 3, 2005; In Final Form: May 13, 2006

Two new molecular dyads, comprising pyrromethene (bodipy) and 2,2′:6′,2″-terpyridine (terpy) subunits, have been synthesized and fully characterized. Absorption and fluorescence spectral profiles are dominated by contributions from the bodipy unit. Zinc(II) cations bind to the vacant terpy ligand to form both 1:1 and 1:2 (cation:ligand) complexes, as evidenced by X-ray structural data, NMR and spectrophotometric titrations. Attachment of the cations is accompanied by a substantial decrease in fluorescence from the bodipy chromophore due to intramolecular electron transfer across the orthogonal structure. At low temperature, nuclear tunneling occurs and the rate of electron transfer is essentially activationless. However, activated electron transfer is seen at higher temperatures and allows calculation of the corresponding reorganization energy and electronic coupling matrix element. In both cases, charge recombination is faster than charge separation.

Introduction

Electron-transfer processes are ubiquitous in chemistry, biology, medicine and biochemistry. Because of a solid theoretical framework, the many factors that combine to control the rate of electron transfer are known and can be manipulated by synthetic means. Of particular importance in terms of optimizing the rate of intramolecular electron transfer are the mutual orientation of donor and acceptor species[1] and their structural relationship to any bridging unit connecting the terminal reactants.[2] This facet of electron-transfer theory is hidden within the electronic coupling matrix element that describes the extent of orbital overlap between the various species. Such considerations can be used to suggest that the rate of electron transfer should be at a minimum when the reactants are held at an orthogonal geometry,[3] even if their separation distance is short. Quantum chemical calculations[4] indicate that, in certain cases, orbital overlap can approach zero when the reactants adopt an orthogonal arrangement but experimental work suggests otherwise. Thus, rapid light-induced electron transfer has been observed in simple molecular dyads believed to display orthogonal structures.[5] Of course, it is difficult to ensure that the geometry remains free from thermal fluctuations[6] and that nuclear tunneling does not contribute to the overall electron-transfer process, especially at low temperature.[7] Even so there are some interesting cases of fast electron transfer across orthogonal geometries in short-range molecular dyads that merit detailed theoretical examination.

Here, we attempt to extend the field by describing the photophysics of a molecular dyad based on a bora-3*a*,4*a*-diaza-*s*-indacene (bodipy) dye bearing a vacant coordination site.[8,9] Many examples of bodipy derivatives have been developed as chromogenic reagents,[10,11] chemioluminescent materials,[12] electroluminescent compounds[13] and laser dyes[14] and these materials are known to be highly fluorescent under ambient conditions.[15] The coordination site, which is held close to the dye molecule, is 2,2′:6′,2″-terpyridine (terpy); this is a well-known, universal chelating agent that will complex an inordinately wide range of cations from solution.[16] On coordination of zinc(II) cations, the reduction potential of the terpy ligand shifts to a much less negative potential such that the possibility of intramolecular electron transfer increases markedly.[16] Other examples are known whereby supramolecular approaches are used to assemble photoactive dyads from their constituent parts.[17] This is an attractive route to the construction of versatile optoelectronic devices that eliminates unnecessary synthesis. It also provides a means by which to effect self-repair of a damaged module; a difficult feature with purely covalent molecular edifices. In the first instance, we have sought to evaluate the ability of the self-assembled structure to undergo fast electron transfer across the essentially orthogonal geometry imposed by cation complexation.[18]

Experimental Methods

Structural formulas for the molecular systems studied herein are given in Figure 1. The free ligands **1a** and **2a** were prepared,

* Corresponding author. E-mail: anthony.harriman@ncl.ac.uk; ziessel@chimie.u-strasbg.fr.
† University of Newcastle.
‡ Institut de Chimie des Substances Naturelles.
§ Université Louis Pasteur.

10.1021/jp054992c CCC: $33.50
Published on Web 06/14/2006

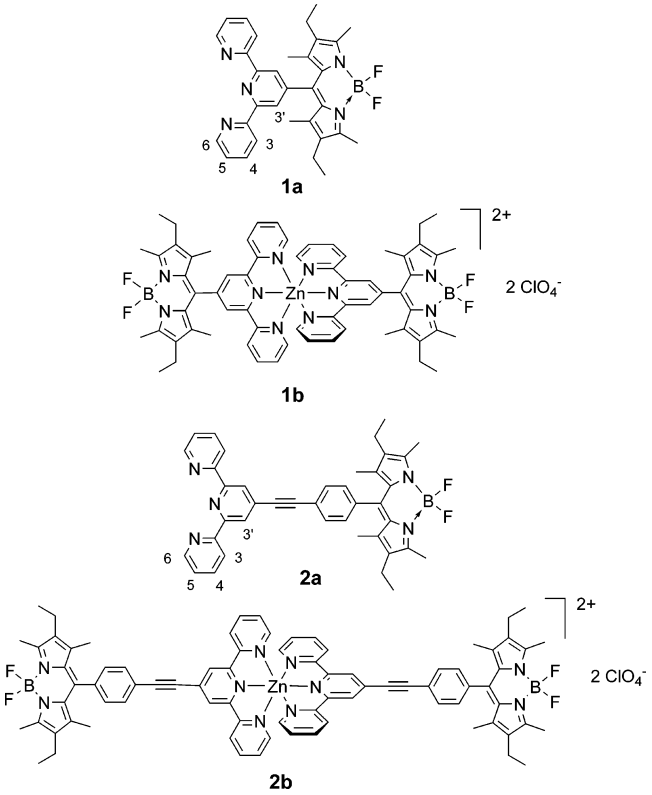

Figure 1. Structural formulas for the bodipy-based chelating agents used in this work and the corresponding 1:2 complexes formed with zinc(II) cations.

purified and characterized according to a literature procedure.[9b] The corresponding zinc(II) complexes were prepared as follows:

Bis{4,4-Difluoro-8-(2′:2″;6″:2‴terpyridin-4″-yl)-1,3,5,7-tetramethyl-2,6-diethyl-4-bora-3*a*,4*a*-diaza-*s*-indacene}zinc-(II) bis(hexafluorophosphate) (1b). To a solution of 4,4-difluoro-8-(2′:2″;6″:2‴terpyridin-4″-yl)-1,3,5,7-tetramethyl-2,6-diethyl-4-bora-3*a*,4*a*-diaza-*s*-indacene (0.05 g, 0.095 mmol) in CH_2Cl_2 (5 mL) was added a methanolic solution of zinc perchlorate hexahydrate (0.018 g, 0.0475 mmol). The orange solution immediately turned deep red and was stirred for 1 day. Slow diffusion of diethyl ether into the mixture afforded the title compound as red crystals (0.048 g, 77%). ^{1}H NMR (300 MHz, CD_3COCD_3): δ = 1.04 (t, 12H, ^3J = 7.5 Hz), 1.82 (s, 12H), 2.45 (q, 8H, ^3J = 7.5 Hz), 2.61 (s, 12H), 7.66 (m, 4H), 8.14 (d, 4H, ^3J = 4.9 Hz), 8.36 (td, 4H, ^3J = 7.9 Hz, ^4J = 1.1 Hz), 9.04 (d, 4H, ^3J = 8.1 Hz), 9.33 (s, 4H). ^{13}C{^{1}H} NMR (100.6 MHz, CD_3COCD_3): δ = 12.3 (CH_3), 12.8 (CH_3) 14.5 (CH_3), 17.0 (CH_2), 124.6 (CH), 124.9 (CH), 128.6 (CH), 129.7, 129.8, 134.3, 135.1, 136.2, 138.5, 142.1 (CH), 144.8, 148.1, 148.4, 148.5 (CH), 151.3, 153.1, 156.0. MS (FAB$^+$, mNBA): *m*/*z* (%) = 1235.2 [M − ClO_4], 567.2 (20) [M − 2(ClO_4)]$^{2+}$. Anal. Calcd for $C_{64}H_{64}N_{10}O_8B_2Cl_2F_4Zn$: 57.57; H, 4.83; N, 10.49. Found: C, 57.40; H, 4.63; N, 10.21.

Bis{4′-{ethynylphenyl-4‴-[4″″,4⁗-Difluororo-8⁗-(1⁗,3⁗,5⁗,7⁗-tetramethyl-2⁗,6⁗-diethyl-4⁗-bora-3⁗*a*,4⁗*a*-diaza-*s*-indacene)]}-2:2′;6′:2″−terpyridine}zinc-(II) bis(hexafluorophosphate) (2b). To a stirred solution of 4′-{ethynylphenyl-4‴-[4⁗,4⁗-difluororo-8⁗-(1⁗,3⁗,5⁗,7⁗-tetramethyl-2⁗,6⁗-diethyl-4⁗-bora-3⁗*a*,4⁗*a*-diaza-*s*-indacene)]}-2:2′;6′:2″terpyridine (0.05 g, 0.0787 mmol) in CH_2Cl_2 (3 mL) was added zinc perchlorate hexahydrate (0.015 g, 0.0393 mmol) in methanol. The solution turned rapidly from orange to deep red and a red precipitate appeared slowly. The mixture was stirred for 1 day. The precipitate was recovered by centrifugation and washed twice with diethyl ether. No further purification was needed to obtain the pure target complex as a red powder (0.58 g, 98%). ^{1}H NMR (300.13 MHz, CD_3CN): δ = 1.01 (t, 12H, ^3J = 7.5 Hz, CH_3), 1.43 (s, 3H), 2.36 (q, 8H, ^3J = 7.4 Hz), 2.50 (s, 12H), 7.42−7.46 (m, 4H), 7.57 (d, 4H, ^3J = 8.3 Hz), 7.85 (d, 4H, ^3J = 4.9 Hz), 7.94 (d, 4H, ^3J = 8.3 Hz), 8.18 (td, 4H, ^3J = 7.8 Hz, ^4J = 1.2 Hz), 8.58 (d, 4H, ^3J = 8.1 Hz), 8.92 (s, 4H). ^{13}C{^{1}H} DEPT NMR (75.4 MHz, CD_3CN): δ = 12.4 (CH_3), 12.9 (CH_3) 14.9 (CH_3), 17.6 (CH_2), 87.6, 99.3, 122.7, 124.2 (CH), 126.4 (CH), 128.9 (CH), 130.5(CH), 131.3, 134.1 (CH), 134.5, 138.8, 139.7, 140.1, 140.4, 142.5 (CH), 148.4, 149.3 (CH), 150.8, 155.3. MS (FAB$^+$, mNBA): *m*/*z* (%) = 1435.2 [M − ClO_4], 667.2 (10) [M − 2(ClO_4)]$^{2+}$. Anal. Calcd for $C_{80}H_{72}N_{10}O_8B_2Cl_2F_4Zn$: 62.58; H, 4.73; N, 9.12. Found: C, 62.30; H, 4.56; N, 8.81.

Crystal Data for the [Zn(1a)$_2$](ClO_4)$_2$ Complex (1b). Crystallization of the complex gave microscopic diamond-shaped plates, about 60 μm thick, the largest dimension never exceeding 80 μm. A single crystal was used for the complete X-ray diffraction data recording at the DW-32 station[19] on the wiggler line at the synchrotron DCI (Orsay) using the rotation method on a MAR−RESEARCH (F-345 mm) image plate camera. Data processing was done with the DENZO program.[20] Intensities were corrected as usual from Lorentz polarization and beam decrease and then reduced to a unique set of amplitudes using the SCALA and TRUNCATE programs from the CCP4 suite.[21] The structure was solved by direct methods (SHELX-S86)[22] and was refined on F2 for all reflections by least-squares methods using SHELXL-93.[23] [$ZnC_{64}N_{10}H_{64}$]$^{2+}$, 2(ClO_4)$^-$, $(C_2H_5)_2O$, CH_3OH, M = 1441.30, triclinic, space group $P\bar{1}$, a = 9.376(4) Å; b = 18.932(8) Å; c = 20.837(8) Å; α = 96.88(4)°, β = 101.14(4)°, γ = 104.49(4)°, V = 3458(3) Å^3, Z = 2, d_c = 1.384 g cm^{-3}, F(000) = 1504, μ = 0.509 mm^{-1}, λ = 0.947 Å. The asymmetric unit consists of one Zn(II) cation complex, two ClO_4^- anions, one diethyl ether and one methanol. Diethyl ether and methanol are present as solvates and contribute to the cohesion of crystal packing. All hydrogen atoms, including those residing on the methanol solvate, were located by difference Fourier syntheses. They were modeled at their theoretical positions using an isotropic thermal factor equal to 1.2 times that of the bonded atom and introduced in the refinement cycles. The final conventional R is 0.0398 for 6102 observed reflections with $F_o > 4\sigma(F_o)$ and 905 parameters, and 0.040 for all data, $wR(F_2)$ = 0.105 for all, $w = 1/[\sigma^2(F_o)^2 + (0.0641P)^2 + 5.41P]$, where $P = (F_o^2 + 2F_c^2)/3$. The largest difference peak and hole are 0.4 and −0.49 e Å^{-3}. A summary of the important crystallographic data is given in the Supporting Information (Table S1). A selection of bond lengths and angles is presented in Tables S2 and S3 in the Supporting Information. The ORTEP plot of the [Zn(II)] complex is shown in Figure 2. Crystal data and selected experimental details, a list of atomic coordinates, bond lengths, bond angles, anisotropic thermal parameters of non-hydrogen atoms, and atomic coordinates of hydrogen atoms are provided as Supporting Information.

Spectroscopic Studies. Spectrophotometric grade solvents were purchased from Aldrich Chemicals Co. and used as received. Absorption and fluorescence spectra were recorded using a Hitachi U3310 spectrophotometer and a Hitachi F4500 spectrofluorometer, respectively. Low-temperature emission spectra were taken using an Oxford Optistat cryostat controlled by an Oxford Instruments temperature controller. Temperature-dependent emission spectra were collected from 77 K to room temperature in 10° intervals. The system was allowed to

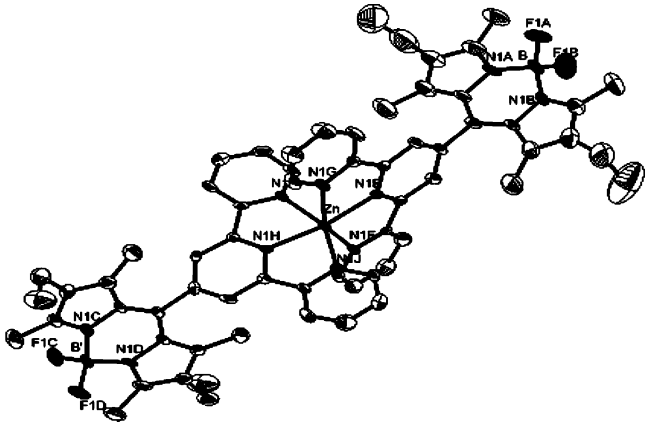

Figure 2. ORTEP diagram for **[**Zn(**1a**)$_2$](ClO$_4$)$_2$ showing the atom-labeling scheme. Thermal ellipsoids are plotted at the 30% level. Structural data have been deposited with the Cambridge Crystallographic Data Centre (CCDC) under the depository number CCDC 270125.

equilibrate for 15 min between each reading. Emission quantum yields were measured in N_2-purged methanol relative to Rhodamine 6G.[24] Fluorescence lifetimes were recorded using the phase modulation method on an Yvon-Jobin Fluorolog Tau-3 Lifetime System with the instrumental response function being measured against a solution of Ludox in distilled water. Fluorescence titrations were made by addition of small aliquots of a 1 mM Zn(ClO$_4$)$_2$ solution to dilute solutions (ca. 1 μM) of the free ligand. A minimum of 30 additions was made for each titration, and measurements were repeated at least twice. Data analysis was made with SPECFIT for absorption spectral measurements or with purpose-written software for fluorescence studies.

Electrochemical studies were made by cyclic voltammetry using a conventional 3-electrode system controlled by an HCH Instruments Electrochemical Analyzer connected to a PC. The working, counter and reference electrodes used were glassy carbon, Pt wire and Ag/AgCl, respectively. Solutions contained the ligand (1 mM) and tetra-*N*-butylammonium tetrafluoroborate (0.1 M) as supporting electrolyte. All solutions were deoxygenated by purging with dry N_2 prior to the experiment. Ferrocene was used as internal reference. Molecular orbital calculations were made on energy-minimized conformations calculated by Gaussian 03[25] using the parametrized semiempirical AM1 method.[26] Such AM1 calculations are far from definitive for boron-containing compounds but have been found to adequately model cyclic boron ethers.[27] Parameters for boron[28a] and zinc[28b] were taken from the literature. Closely comparable results were obtained from extended Hückel calculations also made with Gaussian 03.[25]

Flash photolysis studies were made with a variety of instruments. An Applied Photophysics LKS60 was used for ns studies. Excitation was made with 4 ns pulses at 532 nm delivered with a frequency-doubled, Q-switched Nd:YAG laser whereas detection was made at 90° using a pulsed, high-intensity Xe arc lamp. The signal was detected with a fast response PMT after passage through a high radiance monochromator. Transient differential absorption spectra were recorded point-by-point with 5 individual records being averaged at each wavelength. Kinetic measurements were made after averaging 50 individual records using global analysis methods. The sample was purged with N_2 before use. For some studies, iodomethane (10% v/v) was added before photolysis. The laser intensity was calibrated by reference to the triplet state of zinc *meso*-tetraphenylporphyrin in deoxygenated toluene. Quantum yield measurements were made after sensitization with benzophenone in acetonitrile over a wide range of laser intensities. For these studies, the triplet quantum yield and T_1-T_n molar absorption coefficient at 525 nm for benzophenone were taken as 1.0 and 6500 M^{-1} cm^{-1}, respectively.[29]

Improved time resolution was achieved with a mode-locked, frequency-doubled Nd:YAG laser (fwhm = 20 ps). The excitation pulse was passed through a Raman shifter to isolate the required wavelength. The monitoring pulse was a white light continuum, delayed with respect to the excitation pulse with a computer-controlled optical delay line. For the former studies, the two pulses were directed almost collinearly through the sample cell. The monitoring pulse was dispersed with a Princeton Instruments spectrograph and detected with a dual-diode array spectrometer. Approximately 150 individual laser shots were averaged at each delay time. Kinetic parameters were derived by overlaying spectra collected at different delay times. All measurements were made with dilute solutions after purging with N_2.

Results and Discussion

Structural Details for the Zinc(II) Complexes. The ^{1}H NMR spectra are typical of a bis(terpyridine)zinc(II) complex in an octahedral environment (Figure 3 and Supporting Information). For each complex, the two ligands are magnetically equivalent because of a 2-fold symmetry axis lying along the B−Zn−B main axis. Assignment of the terpy peaks was made on the basis of 2D NMR studies. A downfield shift of the 3′,5′ protons of the terpy core is observed for both complexes relative to the free ligands and is due to the electron withdrawing effect of the zinc cation. This downfield shift of 0.80 ppm for H3′ is rather strong in the case of **1b**, because the indacene fragment is in close proximity to the terpy subunit. The effect is further illustrated by a 0.2 ppm downfield shift of the phenyl ring AB system of ligand **2a**. A similar effect is observed in the ^{13}C NMR, with an downfield shift of 7 ppm for the chemical shift of the C≡C carbon linked to the terpy unit. Simultaneously, the nearest methyl group on the bodipy fragment is shifted downfield from 1.43 ppm in **1a** to 1.72 ppm in **1b**. It is worth noting that almost no shift is observed for this methyl group in **2a** versus **2b**. In contrast, the 6 and 6″ protons are strongly shielded in both complexes. Coordination causes adoption of an all cis conformation of the nitrogen atoms and a stiffening of the terpy fragment. This forces protons ortho to the N of the external pyridines into the shielding zone of the central pyridine on the opposite terpy, as can be seen in the crystal structure.

The X-ray structure determination of **1b** confirms the anticipated orthogonal arrangement of the terpy and dipyrromethene fragments (Figure 2), which is imposed by the substituents. The dihedral angles between the bodipy [AB] and the terpy [EFG] fragments, and between the bodipy [CD] and the terpy [HIJ] units, respectively, are 86.0(1)° and 82.8(1)°. The two diazaindacene fragments are essentially planar: the maximum deviation from the least-squares mean plane of the 12 atoms of the 2 indacene groups is ±0.048(3) Å for [AB] and ±0.048(3) Å for [CD], and the dihedral angles of the pyrrole fragments A and B are 3.4 (2)° and 2.1(3)° for C and D. The bond distances for the indacene fragments are in good agreement with related systems reported in the literature. This is also true for the B site; the average B−N bond length of 1.54 Å and average B−F bond length of 1.38 Å.[16,30,31] Slight distortion within the two terpy ligands is observed, due to twisting around the interannular C−C bond. The tilt observed within the terpy subunit is due to the need to accommodate the cation; important

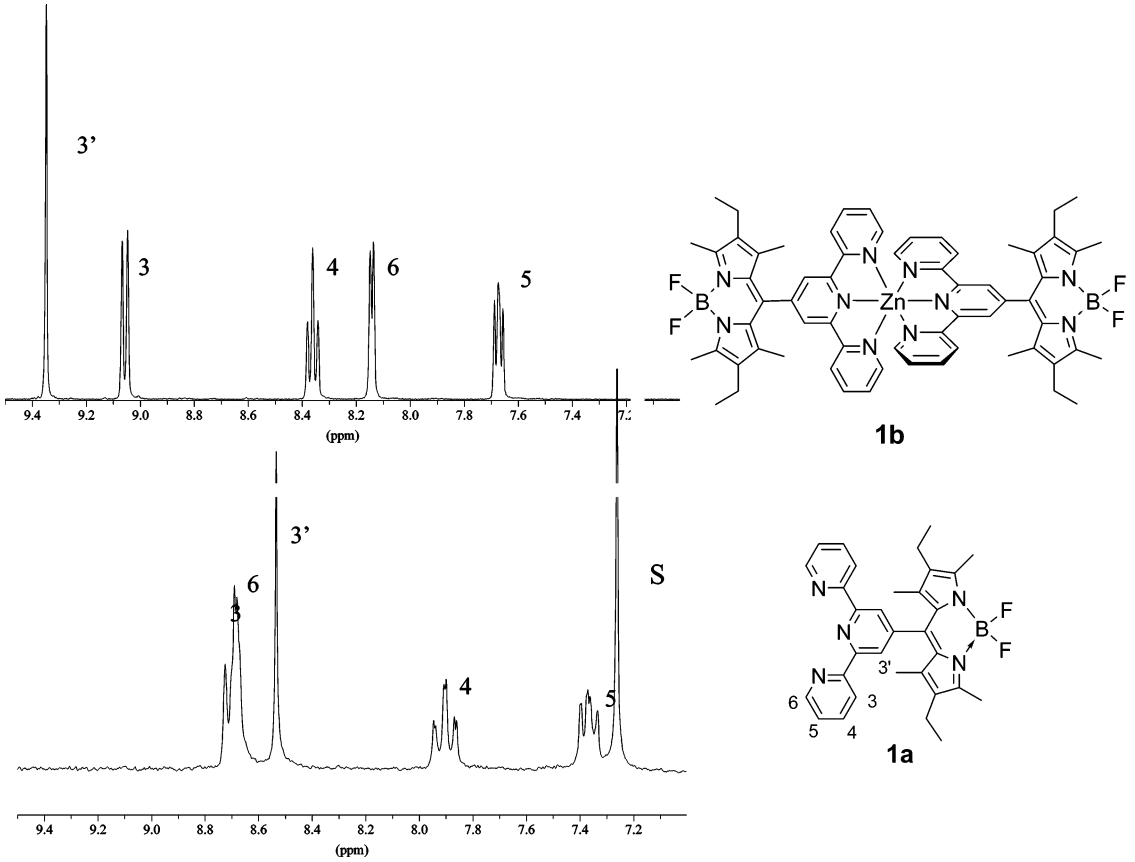

Figure 3. ^{1}H NMR spectra of ligand **1a** (bottom) and complex **1b** (top), respectively, in acetone-d_6 and $CDCl_3$. For the sake of clarity, only the aromatic regions of the spectra are represented. Note that peak attribution is derived from the 2D experiments.

dihedral angles are 18.0(1)° between the pyridine H ring and pyridine J ring, 10.8(2)° between H and J, 8.5(2)° between F and E, and 6.9(2)° between E and G.

The coordination sphere around the cation reveals a distorted octahedral arrangement. The bond lengths and angles around the Zn(II) center are in good agreement with the values found in similar complexes.[32] The terpy ligands bind the metal center via their three pyridine N atoms. The two central pyridine N atoms lie opposite each other and the two terpy units are strictly orthogonal. The Zn−N bond lengths are shorter [2.096(2) Å and 2.101(3) Å] for the central pyridines than for the outer pyridines [range value 2.16−2.21 Å]. This finding confirms distortion of the octahedral geometry and slight axial compression.

Photophysical Studies. The absorption spectrum of **1a** in acetonitrile is shown in Figure 4. This spectrum, which is essentially a superposition of the individual spectra, is dominated by the strong $S_0 \rightarrow S_1$ transition centered (λ_{MAX}) at 525 nm ($\epsilon_{MAX} = 72\,000\ M^{-1}\ cm^{-1}$) and a weaker, broad $S_0 \rightarrow S_2$ band centered at 375 nm.[33] Both transitions are localized on the bodipy chromophore, with the terpy unit contributing toward absorption around 290 nm.[34] Fluorescence is readily observed in fluid solution at ambient temperature and shows good mirror symmetry with the $S_0 \rightarrow S_1$ transition (Figure 4). The small Stokes' shift (ca. 550 cm^{-1}) implies there is little change in geometry or polarity between ground and excited states and the corrected excitation spectrum shows excellent agreement with the absorption spectrum recorded over the visible and near-UV region. There are no indications for pronounced electronic communication between the bodipy and terpy subunits. The electronic isolation of the two subunits is further supported by the energy-minimized geometries calculated using the AM1 method, which clearly show the orthogonal geometry between the two subunits. Molecular orbital calculations show that both HOMO and LUMO are localized on the bodipy fragment (see Supporting Information). Cyclic voltammetry indicates reversible one-electron processes associated with oxidation (E_{OX} = 1.11 V vs SSCE) and reduction (E_{RED} = −1.14 V vs SSCE) of the bodipy unit and a separate reduction of the terpy fragment (E_{RED} = −1.74 V vs SSCE). Solutions of **1a** showed no degradation on prolonged storage, although fresh samples were prepared for each experiment. Compound **2a**, which has increased separation between the bodipy and terpy subunits,

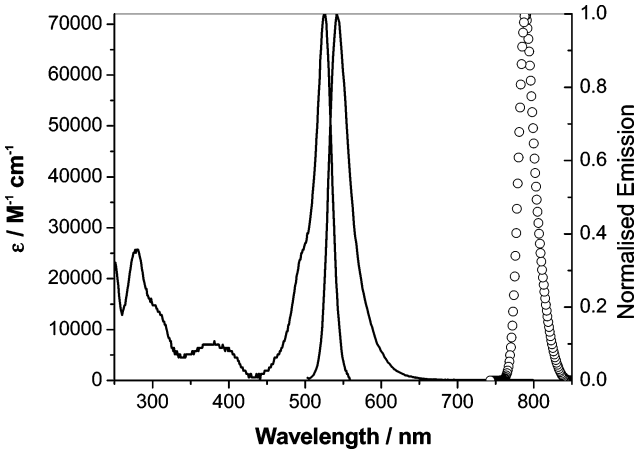

Figure 4. Absorption and fluorescence spectra recorded for **1a** in acetonitrile at room temperature. (○) Low-temperature phosphorescence spectrum recorded in ethanol containing 10% v/v iodoethane.

TABLE 1: Photophysical and Electrochemical Properties Recorded for the Bodipy-based Dyes in Dilute Acetonitrile Solution at 20 °C

property	**1a**	**2a**
λ_{MAX}/nm	525	522
ϵ_{MAX}/M^{-1} cm^{-1}	72 000	60 000
λ_{FLU}/nm[a]	541	538
Φ_F	0.68	0.64
τ_S/ns	3.8	4.0
k_{RAD}/s^{-1} [b]	1.6×10^8	1.3×10^8
λ_{PHO}/nm[c]	785	750
τ_{PHO}/ms[d]	1.2	1.2
τ_T/μs[e]	55	30
E_{OX}/V vs SSCE[f]	+1.11	+1.12
E_{RED}/V vs SSCE[g]	−1.14	−1.13

[a] Fluorescence maximum. [b] Radiative rate constant calculated from the Strickler−Berg expression. [c] Phosphorescence maximum measured at 77 K. [d] Phosphorescence lifetime measured in deoxygenated ethanol containing 10% v/v iodoethane. [e] Triplet lifetime measured in deoxygenated solution. [f] Oxidation potential for the bodipy dye. [g] Reduction potential for the bodipy dye.

shows similar absorption and fluorescence spectral properties (see Supporting Information). Key information is summarized in Table 1.

The fluorescence quantum yield (Φ_F) and excited-singlet-state lifetime (τ_S) of **1a** in deoxygenated acetonitrile solution at room temperature were found to be 0.68 ± 0.03 and 3.8 ± 0.1 ns, respectively. These values are comparable to those found for related bodipy dyes[35,36] and allow calculation of the radiative rate constant (k_{RAD}) as 1.8×10^8 s^{-1}; this value agrees well with that calculated from the Strickler−Berg equation ($k_{RAD} = 1.6 \times 10^8$ s^{-1}). Weak phosphorescence could be observed in a butyronitrile glass at 77 K containing 10% v/v iodoethane, with the peak being located at 785 nm (Figure 4). The phosphorescence lifetime (τ_P) was found to be 1.2 ± 0.1 ms under these conditions. The triplet excited state was barely detectable by nanosecond laser flash photolysis following excitation at 355 nm at room temperature unless a heavy atom solvent was added. Thus, excitation of **1a** in deoxygenated acetonitrile containing 10% v/v iodoethane at room temperature gave rise to a transient differential absorption spectrum showing weak absorbance on either side of the $S_0 \rightarrow S_1$ bleaching signal. This transient species decays via first-order kinetics, with a lifetime of 55 ± 5 μs, and is assigned to the triplet excited state. The same transient species is observed after sensitization with benzophenone (Figure 5) and it is concluded that the quantum yield for direct intersystem crossing in **1a** is <0.001. Compound **2a** shows similar behavior (Table 1). It should be noted that the results collected for **1a** and **2a** are in good accord with earlier studies made with related bodipy dyes, although detection of low-temperature phosphorescence has not been reported before.[16]

The excited-singlet-state lifetime depends weakly on temperature, in line with the energy-gap law.[37] Thus, the fluorescence yield and lifetime recorded for **1a** increase linearly by ca. 30% on cooling from room temperature to 77 K in ethanol. The change (i.e., ca. 40%) for **2a** is comparable. There were no obvious changes in spectral profile or emission maximum over this temperature range. Likewise, no obvious effects of concentration quenching were observed for either dye.[38]

Titration with Zinc(II) Cations. Addition of zinc(II) to a solution of **1a** in acetonitrile solution causes the appearance of new absorption bands around 330 nm and a 7 nm red shift of the $S_0 \rightarrow S_1$ transition (Figure 6). Comparison with an authentic sample shows that the new absorption bands are due to formation of zinc(II) bis(terpyridine), in good agreement with the X-ray data. Compound **2a** also undergoes complexation with

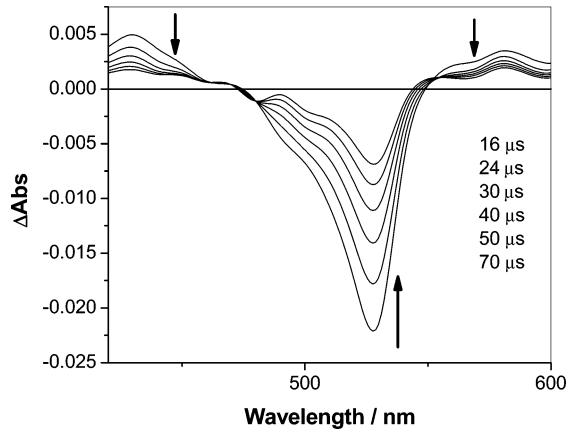

Figure 5. Transient differential absorption spectrum recorded for the triplet excited state of **1a** in deoxygenated acetonitrile solution. Formation of the triplet state was sensitized by benzophenone.

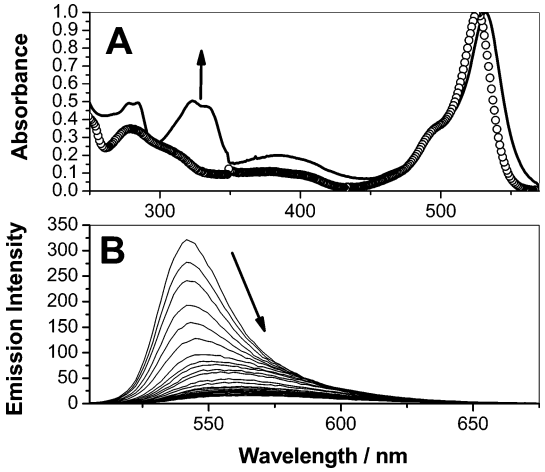

Figure 6. (A) Absorption spectrum recorded after addition of a 40-fold molar excess of $Zn(ClO_4)_2$ to a solution of **1a** in acetonitrile solution: (○) before addition of salt; (—) after addition of salt (represents the spectrum of **1b**). (B) Fluorescence spectral profiles recorded after successive additions of $Zn(ClO_4)_2$ (0−32 mM) to a solution of **1a** (10 μM) in acetonitrile solution.

the added cation but there is no red shift for the $S_0 \rightarrow S_1$ transition. Presumably, the shift seen for **1a** arises from an electronic effect that is switched-off by the increased separation in **2a**. The presence of zinc(II) causes a drastic decrease in fluorescence for both **1a** and **2a**. For **2a**, there is a progressive loss of fluorescence upon successive addition of cation until a plateau is reached (see Supporting Information). The limiting value corresponds to a 25-fold reduction in fluorescence for **2a**. For **1a**, however, fluorescence quenching is accompanied by a slight shift of the fluorescence band to 548 nm, in line with the absorption spectral change (Figure 6). The quantum yield for this latter band, measured at the plateau point, is ca. 0.020 ± 0.005. The appearance of the plateau region for both compounds is indicative of complexation between the reagents, and on the basis of the absorption spectral changes and X-ray structural data it is presumed that the cation coordinates to the vacant terpy site. This latter point is emphasized by the fact that fluorescence from a bodipy dye lacking the terpy fragment is unaffected by the presence of excess zinc(II) perchlorate.

Fitting the titration data requires the stepwise formation of 1:1 and 1:2 (metal:ligand) complexes.[39] Stability constants (β) were derived from both absorption and fluorescence titrations and found to agree reasonably well (Table 2). In each case, the

TABLE 2: Properties Relating to the Corresponding Zinc(II) Complexes Recorded in Acetonitrile Solution at 20 °C

property	1b	2b
$\log \beta_{11}$[a]	7.4 (8.2)	7.0
$\log \beta_{12}$[a]	12.3 (14.3)	11.5
E_{OX}/V vs SSCE[b]	1.11	1.13
E_{RED}/V vs SSCE[c]	−0.89 (−0.96)	−1.05 (−0.93)
τ_S/ps[d]	150	200
τ_T/μs[e]	72 (8)	14 (17)
$\Delta G°$/kJ mol^{-1}	−17.8	−23.7
k_Q/s^{-1}	6.3×10^9	4.8×10^9
$\Delta G^{\#}$/kJ mol^{-1}	16.9	15.3
λ/eV[f]	1.04	1.15
V_{DA}/cm^{-1} [g]	160	98
k_{ACT}/s^{-1} [h]	4.1×10^8	NA

[a] Overall stability constant measured by fluorescence titration with the value in parentheses referring to the corresponding measurement made by absorption spectroscopy. [b] Oxidation potential for the bodipy unit measured in the presence of a 10-fold molar excess of $Zn(ClO_4)_2$. [c] Reduction potential for the bodipy unit measured in the presence of a 10-fold molar excess of $Zn(ClO_4)_2$ with the value in parentheses referring to the corresponding reduction process for the Zn−terpy unit. [d] Singlet lifetime. [e] Triplet lifetime measured in deoxygenated acetonitrile with the value in parentheses referring to the corresponding value found in the presence of 10% v/v iodoethane. [f] The reorganization energy for activated electron transfer. [g] Electronic coupling matrix element for activated electron transfer. [h] Activationless rate constant for electron transfer observed at low temperature.

stability constant ($\log \beta_{12}$) for the 1:2 complex was found to somewhat less than twice the value for the 1:1 complex ($\log \beta_{11}$), showing the absence of positive cooperativity. There were no significant differences between the two complexes. Semiempirical calculations resulted in a lowest-energy structure for the 1:2 complex formed from **1a** that was in good agreement with the X-ray results (see Supporting Information). This structure has the proximal bodipy and terpy units held in an orthogonal geometry, due to steric interactions between the methyl groups on bodipy and protons on terpyridine. Similar calculations made for the 1:2 complex obtained from **2a** also require an orthogonal geometry as the lowest-energy conformation.

Fluorescence Quenching by Bound Cation. Steady-state fluorescence spectroscopy indicates that the excited singlet state of the bodipy dye is extensively quenched on complexation of the terpy unit by zinc(II) cations, for both **1a** and **2a**. Singlet-state lifetimes measured for the 1:2 complexes by time-resolved fluorescence spectroscopy in acetonitrile solution at room temperature are 150 ± 12 and 200 ± 15 ps, respectively, for **1a** and **2a**. As such, the first-order rate constants for fluorescence quenching in these systems can be calculated as 6.3×10^9 and 4.8×10^9 s^{-1}, respectively, for **1a** and **2a** at room temperature (Table 2). It is interesting to note that the elongation of the molecule (by 6.9 Å) inherent to **2a** has only a modest effect on the rate of quenching. Cyclic voltammetry indicates that, whereas the bound cation has no effect on oxidation of the bodipy dye, a new peak appears on reductive scans. This quasi-reversible peak, which is attributed to one-electron reduction of the Zn−terpy complex, is characterized by half-wave potentials of −0.96 and −0.93 V vs SSCE, respectively, for **1b** and **2b** (Table 2).[40] As such, light-induced electron transfer from the singlet state of the bodipy dye to the appended Zn−terpy complex is thermodynamically feasible in both cases (Table 2), even after allowing for electrostatic effects.[41] The triplet excited state is unlikely to enter into electron-transfer processes under these conditions because ΔG^0_{CS} is strongly positive for both systems. The cyclic voltammograms also indicate that reduction of the bodipy unit is made easier by coordination of the zinc(II) cation, especially in the case of **1b**, due to an electrostatic effect.

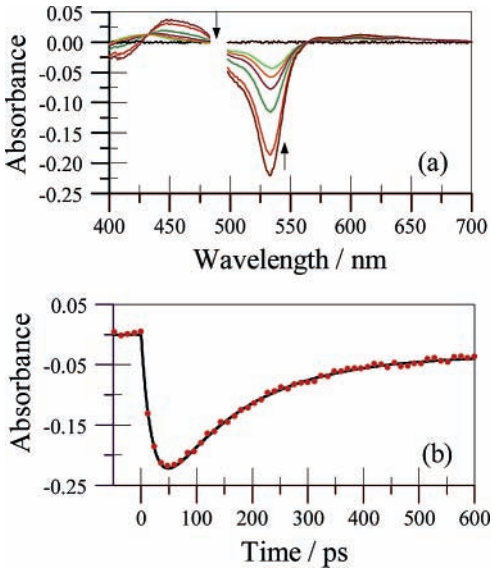

Figure 7. (a) Transient differential absorption spectra recorded after laser excitation of **1b** in deoxygenated acetonitrile: delay times are 0, 50, 100, 200, 300, 400 and 600 ps. (b) Kinetic trace recorded at 540 nm.

Laser flash photolysis studies made with ns temporal resolution showed that the bodipy triplet state was present after the excitation pulse. The yield of the triplet, although significantly higher than that recorded in the absence of zinc(II) perchlorate, was far from quantitative because addition of iodoethane (10% v/v) caused a further enhancement. The lifetime of the triplet state recorded for **1a** in the presence of excess $Zn(ClO_4)_2$ was 70 μs; this value decreased to 8 μs on addition of iodoethane. Similar behavior was noted for **2b** (Table 2). In both cases, the transient absorption spectra remained indistinguishable from those recorded prior to addition of zinc(II) perchlorate. These results indicate that cation-induced fluorescence quenching enhances intersystem crossing to the locally excited triplet state but that this process is in competition with nonradiative decay to re-form the ground state.

Excitation of **1b** in deoxygenated acetonitrile with a 20-ps laser pulse results in formation of the bodipy-localized excited singlet state (Figure 7).[42] This species shows pronounced bleaching of the ground-state $S_0 \rightarrow S_1$ absorption band and weak absorption at higher energies. Recovery of the ground state occurs by way of first-order kinetics with a lifetime of 150 ± 10 ps but about 10% of the bleaching remains after several nanoseconds. No other transient species are observed and, in particular, no absorptions are formed that could be assigned to the bodipy π-radical cation.[43] Our understanding of the transient absorption records is that the excited singlet state is quenched due to intramolecular electron transfer from dye to the Zn−terpy unit.[44] Charge recombination occurs on a much faster time scale than charge separation and leads to a mixture of the ground state (ca. 90%) and the bodipy triplet state (ca. 10%). It was found that **2b** behaves in a similar fashion and does not lead to formation of a long-lived charge-separated state.

$$k_Q\sqrt{T} = \frac{2\pi}{\hbar}\frac{|V_{DA}|^2}{\sqrt{4\pi k_B \lambda}}\exp\left(-\frac{\Delta G^{\#}}{k_B T}\right)$$

$$\Delta G^{\#} = \frac{(\Delta G^0 + \lambda)^2}{4\lambda} \quad (1)$$

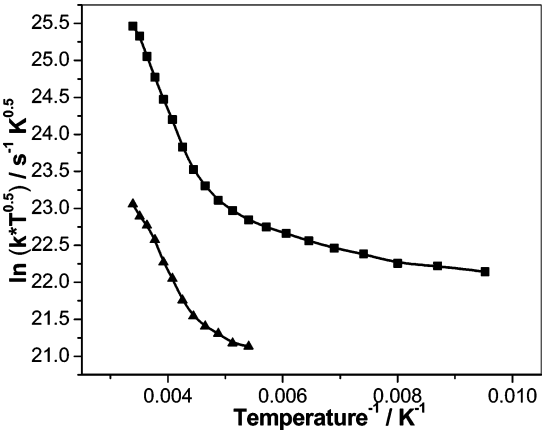

Figure 8. Effect of temperature on the rate constants for decay of the excited singlet states of **1b** (■) and **2b** (▲) in deoxygenated butyronitrile solution. The experimental data are plotted according to eq 1.

The rate of fluorescence quenching (k_Q) was found to decrease progressively with decreasing temperature over a wide range (Figure 8). On the assumption that quenching is due to intramolecular electron transfer, the activation energy ($\Delta G^{\#}$) was determined from the linear regions of Marcus-type rate vs driving force plots (eq 1).[45] The derived $\Delta G^{\#}$ values are 16.9 and 15.3 kJ mol^{-1}, respectively, for **1b** and **2b**. From these values, it becomes possible to calculate the reorganization energies (λ) accompanying electron transfer (Table 2). The derived values, which contain contributions from both nuclear and solvent terms, are substantial and ensure that charge separation occurs in the normal Marcus region. That λ is larger for the longer analogue seems consistent with a dominant solvent reorganization energy term. The intercepts, which correspond to the limiting rate of electron transfer, can now be used to compute values for the electronic coupling matrix elements (V_{DA}) associated with the electron-transfer event (Table 2).[45] These values appear quite high, although it has to be realized that the reactants are closely spaced. Indeed, for **1b**, electron transfer is considered to proceed along the connecting σ-bond such that the high V_{DA} does not seem unreasonable. For **2b**, electronic coupling is weaker due to the increased separation but it seems that the acetylene bridge provides a good conduit for electrons.[46]

Charge-separated products are not seen and triplet-state formation accounts for only ca. 10% of the total photon balance. Such findings indicate that charge recombination is highly efficient, despite reaction occurring well within the Marcus inverted region. Presumably, this is a consequence of quantum mechanical effects serving to reduce the activation energy for charge recombination.[47] The failure to populate the bodipy triplet state in high yield, despite the lowered energy gap relative to direct charge recombination,[48] is further indication that spin−orbit coupling is ineffective in this class of dye. Note that the cationic nature of the complexes prevents examination of how solvent polarity might affect the various rate constants.

It might be mentioned at this point that biphasic excited-state decay behavior has been noted for a series of bodipy-based artificial light-harvesting arrays.[49] Here, the excitation pulse is believed to lead to two noninterconverting conformers in the excited-singlet-state manifold. The more structurally distorted conformer decays rapidly to re-form the ground state whereas the Franck−Condon state decays more slowly and gives rise to the observed fluorescence. It is possible that both **1b** and **2b** undergo similar structural distortion under illumination but our limited temporal resolution (i.e., 20 ps) showed only single-exponential decay kinetics.

For **1b**, the rate of electron-transfer becomes independent of temperature in a glassy matrix. This effect is attributed to the onset of nuclear tunneling.[7] Such processes are often seen for charge recombination between closely coupled reactants at low temperature but are less common for the corresponding charge-separation reaction. The derived rate constant (k_{ACT}) is relatively high (Table 2) and accounts for about 50% of the total decay of the excited singlet state under these conditions. For **2b**, there is no clear plateau region in the glassy matrix and, in this case, the rate of electron-transfer becomes too slow to resolve from the radiative decay process.

Concluding Remarks

The two new photoactive systems described herein self-assemble in the presence of added zinc(II) cations in such a way that fluorescence from the terminal bodipy dye is extensively quenched due to intramolecular electron transfer.[44] This latter process is activated at high temperature but becomes activationless in a glassy matrix when the reactants are closely coupled. For the shorter analogue, **1b**, electron transfer occurs along the connecting σ-bond and electronic coupling is relatively high. Electron transfer occurs under nonadiabatic conditions, despite the close proximity. Extending the molecular axis, as in **2b**, decreases the extent of electronic coupling but electron transfer is still the dominant means for deactivation of the excited singlet state. Although the triplet excited state of the bodipy dye lies at lower energy than the charge-separated state, charge recombination occurs preferentially to re-form the ground state. In both cases, the rate of charge recombination exceeds that of charge separation such that charge-separated products are not seen in the transient absorption spectral records. Such behavior has been seen before with closely coupled molecular dyads.[5a−c] Charge recombination might be enhanced by preferential localization of the positive charge at the bridgehead meso carbon at the bodipy π-radical cation level or by quantum mechanical effects. It should also be noted that very fast charge recombination has been reported for a bodipy-based dye substituted with an electron-donating unit.[50]

Although triplet-state formation is relatively unimportant as regards deactivation of the charge-separated state, there is still an impressive increase in the rate constant for intersystem crossing (k_{ISC}) relative to the parent bodipy dye. Thus, k_{ISC} for **1a** and **2a** is less than ca. 5×10^5 s^{-1}. For the corresponding Zn−terpy complexes, k_{ISC} increases to around 5×10^8 s^{-1}, i.e., an increase of at least 1000-fold. It has been shown previously[48] that fast intersystem crossing is to be expected for conformations where the nodal planes of the donating and accepting molecular orbitals are approximately perpendicular to each other. Thus, the orthogonal geometries inherent to **1b** and **2b** should give rise to a large spin−orbit coupling matrix element. There is also the realization that the cation provides additional spin−orbital coupling via the heavy-atom effect.[51] The fact that triplet formation does not dominate over charge recombination is considered to be a consequence of the poor spin−orbital coupling properties of the parent dye.

An interesting feature of the present systems is that the Zn−terpy complex acts as a light harvester[49,52] and channels absorbed photons to the bodipy dye, as evidenced by fluorescence excitation spectroscopy. For both **1b** and **2b**, the rate of singlet−singlet energy transfer from the metal complex to the bodipy dye exceeds 5×10^{10} s^{-1}. The most likely mechanism involves Förster-type, dipole−dipole interactions because there is strong

spectral overlap between fluorescence from Zn−terpy and absorption by bodipy and almost optimal orientation of the relevant transition dipoles. The Zn−terpy chromophore absorbs in the spectral region where bodipy is relatively transparent and can be illuminated with good selectivity.

Acknowledgment. We thank the EPSRC (GR/EP/C007727/1), the CNRS, the University of Newcastle and the Université Louis Pasteur for financial support of this work.

Supporting Information Available: Crystallographic information files (CIF) for **1b** and **2b**, ^{1}H NMR spectra for **2a** and **2b**, tables (S1−S3) showing X-ray data and a comparison with the calculated structural data, HOMO and LUMO molecular orbital pictures for the various systems, absorption/emission spectra for **2a**, energy-minimized structures for 2a and 2b, spectrophotometric titration data for stepwise addition of $Zn(ClO_4)_2$ to **2a**. This material is available free of charge via the Internet at http://pubs.acs.org.

References and Notes

(1) (a) Cave, R. J.; Siders, P.; Marcus, R. A. *J. Phys. Chem*. **1986**, *90*, 1436. (b) Sakata, Y.; Imahori, H.; Tsue, H.; Higashida, S.; Akiyama, T.; Yoshizawa, E.; Aoki, M.; Yamada, K.; Hagiwara, K.; Taniguchi, S.; Okada, T. *Pure Appl. Chem*. **1997**, *69*, 1951.

(2) (a) Kurzawa, J.; Schneider, S.; Buber, J.; Gleiter, R.; Clark, T. *Phys. Chem. Chem. Phys*. **2004**, *6*, 3811. (b) Helms, A.; Heiler, D.; McLendon, G. *J. Am. Chem. Soc*. **1991**, *113*, 4325. (c) Osuka, A.; Maruyama, K.; Mataga, N.; Asahi, T.; Yamazaki, I.; Tamai, N. *J. Am. Chem. Soc*. **1990**, *112*, 4958.

(3) Domingue, R. P.; Fayer, M. D. *J. Phys. Chem*. **1986**, *90*, 5141.

(4) (a) Toutounji, M. M.; Ratner, M. A. *J. Phys. Chem. A* **2000**, *104*, 8566. (b) Lappe, J.; Cave, R. J.; Newton, M. D.; Rostov, I. V. *J. Phys. Chem. B* **2005**, *109*, 6610. (c) Amini, A.; Harriman, A. *J. Phys. Chem. A* **2004**, *108*, 1242.

(5) (a) Rubtsov, I. V.; Redmore, N. P.; Hochstrasser, R. M.; Therien, M. J. *J. Am. Chem. Soc*. **2004**, *126*, 2684. (b) Rubtsov, I. V.; Susumu, K.; Rubtsov, G. I.; Therien, M. J. *J. Am. Chem. Soc*. **2003**, *125*, 2687. (c) Redmore, N. P.; Rubtsov, I. V.; Therien, M. J. *Inorg. Chem*. **2002**, *41*, 566. (d) Maus, M.; Rettig, W.; Bonafoux, D.; Lapouyade, R. *J. Phys. Chem. A* **1999**, *103*, 3388. (e) Niemz, A.; Cuello, A.; Steffen, L. K.; Plummer, B. F.; Rotello, V. M. *J. Am. Chem. Soc*. **2000**, *122*, 4798. (f) van Willigen, H.; Jones II, G.; Farahat, M. S. *J. Phys. Chem*. **1996**, *100*, 3312. (g) Jones, G., II; Farahat, M. S.; Greenfield, S. R.; Gosztola, D. J.; Wasielewski, M. R. *Chem. Phys. Lett*. **1994**, *229*, 40. (h) Fukuzumi, S.; Kotani, H.; Ohkubo, K.; Ogo, S.; Tkachenko, N. V.; Lemmetyinen, H. *J. Am. Chem. Soc*. **2004**, *126*, 1600.

(6) Benniston, A. C.; Harriman, A.; Li, P. Y.; Sams, C. A.; Ward, M. D. *J. Am. Chem. Soc*., **2004**, *126*, 13630.

(7) (a) Jortner, J. *J. Chem. Phys*. **1976**, *64*, 4860. (b) Jortner, J. *Biochim. Biophys. Acta* **1980**, *594*, 193. (c) Ohkita, H.; Benten, H.; Anada, A.; Noguchi, H.; Kido, N.; Ito, S.; Yamamoto, M. *Phys. Chem. Chem. Phys.* **2004**, *6*, 3977. (d) May, V.; Kuhn, O. *Charge and Energy Transfer Dynamics in Molecular Systems*; Wiley-VCH: Berlin, 2001.

(8) Haugland, R. P. *Handbook of Molecular Probes and Research Products*, 9th ed.; Molecular Probes, Inc.: Eugene, OR, 2002.

(9) (a) Ulrich, G.; Ziessel, R. *Synlet.* **2004**, 439. (b) Ulrich, G.; Ziessel, R. *J. Org. Chem.* **2004**, *69*, 2070. (c) Ulrich, G.; Ziessel, R. *Tetrahedron Lett.* **2004**, *45*, 1949.

(10) (a) Wagner, R. W.; Lindsey, J. S. *Pure Appl. Chem*. **1996**, *68*, 1373. (b) Rurack, K.; Kollmannsberger, M.; Resch-Genger, U.; Daub, J. *J. Am. Chem. Soc*. **2000**, *122*, 968. (c) Beer, G.; Rurack, K.; Daub, J. *Chem. Commun.* **2001**, 1138. (c) Turfan, B.; Akkaya, E. U. *Org. Lett*. **2002**, *4*, 2857. (d) Gabe, Y.; Urano, Y.; Kikuchi, K.; Kojima, H.; Nagano, T. *J. Am. Chem. Soc*. **2004**, *126*, 3357.

(11) (a) Beer, G.; Niederalt, C.; Grimme, S.; Daub, J. *Angew. Chem., Int. Ed*. **2000**, *39*, 3252. (b) Kollmannsberger, M.; Rurack, K.; Resch-Genger, U.; Rettig, W.; Daub, J. *Chem. Phys. Lett*. **2000**, *329*, 363. (c) Sancenon, F.; Martinez-Manez, R.; Soto, J. *Angew. Chem., Int. Ed*. **2002** , *41*, 1416.

(12) Lai, R. Y.; Bard, A. J. *J. Phys. Chem. B* **2003**, *107*, 5036.

(13) (a) Brom J. M.; Langer, J. L. *J. Alloys Cmpds*. **2002**, *338*, 112. (b) Hepp, A.; Ulrich, G.; Schmechel, R.; von Seggern, H.; Ziessel R. *Synth. Met.* **2004**, *146*, 11.

(14) (a) Chen, T.; Boyer, J. H.; Trudell, M. L. *Heteroatom Chem*. **1997**, *8*, 51. (b) Sathyamoorthi, G.; Wolford, L. T.; Haag, A. M.; Boyer, J. H. *Heteroatom Chem*. **1994**, *5*, 245.

(15) (a) Pardoen, J. A.; Lugtenburg, J.; Canters, G. W. *J. Phys. Chem*. **1985**, 89, 4272. (b) Kollmannsberger, M.; Rurack, K.; Resch-Genger, U.; Daub, J. *J. Phys. Chem.* **1998**, *102*, 10211. (c) Toele, P.; Zhang, H.; Trieflinger, C.; Daub, J.; Glasbeek, M. *Chem. Phys. Lett*., **2003**, *368*, 66.

(16) Goze, C.; Ulrich, G.; Charbonnière, L.; Ziessel, R. *Chem. Eur. J*. **2003**, *9*, 3748.

(17) (a)Harriman, A.; Kubo, Y.; Sessler, J. L. *J. Am. Chem. Soc*. **1992**, *114*, 388. (b) Osuka, A.; Yoneshima, R.; Shiratori, H.; Okada, T.; Taniguchi, S.; Mataga, N. *Chem. Commun.* **1998**, 1567. (c) Sessler, J. L.; Sathiosathan, M.; Brown, C. T.; Rhodes, A.; Wiederrecht, G. *J. Am. Chem. Soc*. **2001**, *123*, 3655. (d) Armaroli, N.; Barigelletti, F.; Calogero, G.; Flamigni, L.; White, C. M.; Ward, M. D. *Chem. Commun.* **1997**, 2181. (e) Ghaddar, T. H.; Castner, S E. W.; Isied, S. *J. Am. Chem. Soc*. **2000**, *122*, 1233.

(18) Sazanovich, I. V.; Kirmaier, C.; Hindin, E.; Yu, L.; Bocian, D. F.; Lindsey, J. S.; Holten, D. *J. Am. Chem. Soc.* **2004**, *126*, 2664.

(19) Fourme, R.; Dhez, P.; Benoit, J. P.; Kahn, R.; Dubuisson, J. M.; Buisson, P.; Frouin, J. *Rev. Sci. Instrum*. **1992**, *63*, 982.

(20) Ottwinosky, Z.; Minor, W. *Methods Enzymol*. **1997**, *276*, 307.

(21) CCP4 Collaboration Computational Project number 4. *Acta Crystallogr*. **1994**, *D50*, 760.

(22) Sheldrick, G. M. *Acta Crystallogr.* **1990**, *A46*, 467.

(23) Sheldrick, G. M. Program for the refinement of crystal structures. Universität Göttingen, 1993.

(24) Olmsted, J., III. *J. Phys. Chem*. **1979**, *83*, 2581.

(25) Frisch, M. J.; Trucks, G. W.; Schlegel, H. B.; Scuseria, G. E.; Robb, M. A.; Cheeseman, J. R.; Montgomery, J. A., Jr.; Vreven, T.; Kudin, K. N.; Burant, J. C.; Millam, J. M.; Iyengar, S. S.; Tomasi, J.; Barone, V.; Mennucci, B.; Cossi, M.; Scalmani, G.; Rega, N.; Petersson, G. A.; Nakatsuji, H.; Hada, M.; Ehara, M.; Toyota, K.; Fukuda, R.; Hasegawa, J.; Ishida, M.; Nakajima, T.; Honda, Y.; Kitao, O.; Nakai, H.; Klene, M.; Li, X.; Knox, J. E.; Hratchian, H. P.; Cross, J. B.; Bakken, V.; Adamo, C.; Jaramillo, J.; Gomperts, R.; Stratmann, R. E.; Yazyev, O.; Austin, A. J.; Cammi, R.; Pomelli, C.; Ochterski, J. W.; Ayala, P. Y.; Morokuma, K.; Voth, G. A.; Salvador, P.; Dannenberg, J. J.; Zakrzewski, V. G.; Dapprich, S.; Daniels, A. D.; Strain, M. C.; Farkas, O.; Malick, D. K.; Rabuck, A. D.; Raghavachari, K.; Foresman, J. B.; Ortiz, J. V.; Cui, Q.; Baboul, A. G.; Clifford, S.; Cioslowski, J.; Stefanov, B. B.; Liu, G.; Liashenko, A.; Piskorz, P.; Komaromi, I.; Martin, R. L.; Fox, D. J.; Keith, T.; Al-Laham, M. A.; Peng, C. Y.; Nanayakkara, A.; Challacombe, M.; Gill, P. M. W.; Johnson, B.; Chen, W.; Wong, M. W.; Gonzalez, C.; Pople, J. A. *Gaussian 03*, revision C.02; Gaussian, Inc.: Wallingford, CT, 2004.

(26) (a) Dewar, M. J. S.; Reynolds, C. H. *J. Comput. Chem*. **1986**, *2*, 140. (b) Dewar, M. J. S.; Zoebisch, E. G.; Healy, E. F. *J. Am. Chem. Soc*. **1985**, *107*, 3902. (c) Dewar, M. J. S.; McKee, M. L.; Rzepa, H. S. *J. Am. Chem. Soc*. **1978**, *100*, 3607. (d) Dewar, M. J. S.; Thiel, W. *J. Am. Chem. Soc*. **1977**, *99*, 4499.

(27) Kuznetsov, V. V. *J. Struct. Chem*. **2001**, *42*, 494.

(28) (a) Dewar, M. J. S.; Jie, C.; Zoebisch, E. G. *Organometallics* **1988**, *7*, 513. (b) Dewar, M. J. S.; Jie, C. *Organometallics* **1988**, *7*, 522.

(29) (a) Carmichael, I.; Hug, G. L. *J. Phys. Chem. Ref. Data* **1986**, *15*, 1. (b) Bensasson, R. V.; Gramain, J.-C. *J. Chem. Soc., Faraday Trans. 1* **1980**, *76*, 1801.

(30) Wan, C.-W.; Burghart, A.; Chen, J.; Bergström, F.; Johanson, L. B.-A.; Wolford, M. F.; Kim, T. G.; Topp, M. R.; Hochstrasser, R. M.; Burgess, K. *Chem. Eur. J*. **2003**, *9*, 4430.

(31) Shen, Z.; Röhr, H.; Rurack, K.; Uno, H.; Spieles, M.; Schulz, B.; Reck, G.; Ono, N. *Chem. Eur. J*. **2004**, *10*, 4853.

(32) (a) Whittle, B.; Horwood, E. L.; Rees, L. H.; Batten, S. R.; Jeffery, J. C.; Ward, M. D. *Polyhedron* **1998**, *17*, 373. (b) Jeitler, J. R.; Turnbull, M. M.; Wikaira, J. L. *Inorg. Chim. Acta* **2003**, *351*, 331. (c) Harvey, M. A.; Baggio, S.; Ibanez, A.; Baggio, R. *Acta Crystallogr.* **2004**, *C60*, 375.

(33) Karolin, J.; Johansson, L. B.-A.; Strandberg, L.; Ny, T. *J. Am. Chem. Soc*. **1994**, *116*, 7801.

(34) (a) Sarkar, A.; Chakravorti, S. *J. Lumin*. **1995**, *63*, 143. (b) Goodall, W.; Williams, J. A. *Chem. Commun*. **2001**, 2514.

(35) (a) Burghart, A.; Kim, H.; Wech, M. B.; Thorensen, L. H.; Reibenspies, J.; Burgess, K. *J. Org. Chem.* **1999**, *64*, 7813. (b) Kim, H.; Burghart, A.; Welch, M. B.; Reibenspies, J.; Burgess, K. *Chem. Commun*. **1999**, 1889. (c) Chen, J.; Reibenspies, J.; Derecskei-Kovacs, A.; Burgess, K. *Chem. Commun*. **1999**, 2501. (d) Rurack, K.; Kollmannsberger, M.; Daub, J. *New J. Chem.* **2001**, *25*, 289. (e) Rurack, K.; Kollmannsberger, M.; Daub, J. *Angew. Chem., Int. Ed.* **2001**, *40*, 385. (f) Shen, Z.; Röhr, H.; Rurack, K.; Uno, H.; Spieles, M.; Schulz, B.; Reck, G.; Ono, N. *Chem. Eur. J*. **2004**, *10*, 4853.

(36) (a) Susdorf, T.; Alvarez, M.; Holzer, W.; Penzkofer, A.; Amat-Guerri, F.; Liras, M.; Costela, A.; Garcia-Moreno, I.; Sastre, R. *Chem. Phys*. **2005**, *312*, 151. (b) Costela, A.; Garcia-Moreno, I.; Gomez, C.; Sastre, R.; Amat-Guerri, F.; Liras, M.; Arbeloa, F. L.; Prieto, J. B.; Arbeloa, I. L. *J. Phys. Chem. A* **2002**, *106*, 7736. (c) Prieto, J. B.; Arbeloa, F. L.; Martinez, V. M.; Lopez, T. A.; Arbeloa, I. L. *Phys. Chem. Chem. Phys.* **2004**, *6*, 4247. (d) Prieto, J. B.; Arbeloa, F. L.; Martinez, V. M.; Arbeloa, L. *Chem. Phys.* **2004**, *296*, 13.

(37) Englman, R.; Jortner, J. *Mol. Phys*. **1970**, *18*, 145.

(38) Dahim, M.; Mizuno, N. K.; Li, X.-M.; Momsen, E. *Biophys. J.* **2002**, *83*, 1511.

(39) Related bodipy dyes have been used in many other fluorescent sensors for cations and neutral species. See for example: (a) Basaric, N.; Baruah, M.; Qin, W.; Metten, B.; Smet, M.; Dehaen, W.; Boens, N. *Org. Biomol. Chem.* **2005**, *3*, 2755. (b) Malval, J.-P.; Leray, I.; Valeur, B. *New J. Chem.* **2005**, *29*, 1089. (c) Gabe, Y.; Urano, Y.; Kikuchi, K.; Kojima, H.; Nagano, T. *J. Am. Chem. Soc.* **2004**, *126*, 3357.

(40) Under the conditions used for cyclic voltammetry, the dominant species will be the 1:2 metal:ligand complex but there will still be residual free ligand. It was not possible to obtain cyclic voltammograms under conditions where the 1:1 complex would dominate the distribution. Note the reduction peaks for the 1:2 complex were reversible.

(41) The thermodynamic driving force for light-induced electron transfer was calculated according to $\Delta G_{CS} = -F[E_{RED} - E_{OX} + E_S - \Delta E_{EE}]$, where E_{RED} is the reduction potential for the Zn−terpy complex, E_{OX} is the oxidation potential for the bodipy dye, E_S is the excitation energy and ΔE_{EE} is a correction for the change in electrostatic energy. This latter term was calculated according to $\Delta E_{EE} = [e^2/4\pi\epsilon_0\epsilon_S R_{DA}]$, where e is the electronic charge, ϵ_0 is the permittivity of free space, ϵ_S is the dielectric constant of the solvent and R_{DA} is the separation distance taken from the computed structures. For the corresponding charge recombination process, $\Delta G_{CR} = -F[E_{OX} - E_{RED} + \Delta E_{EE}]$.

(42) O'Neil, M. P. *Opt. Lett.* **1993**, *18*, 37.

(43) Jones, G., II; Kumar, S.; Klueva, O.; Pacheco, D. *J. Phys. Chem. A* **2003**, *107*, 8429.

(44) (a) Torimura, M.; Kurata, S.; Yamada, K.; Yoko Kamagata, T.; Kanagawa, T.; Kurane, R. *Anal. Sci.* **2001**, *17*, 155. (b) Arbeloa, F. L.; Prieto, J. B.; Martinez, V. M.; Lopez, T. A.; Arbeloa, I. L. *ChemPhysChem* **2004**, *5*, 1762. (c) Kimple, R. J.; De Vries, L.; Tronchere, H.; Behe, C. I.; Morris, R. A.; Farquhar, M. G.; Siderovski, D. P. *J. Biol. Chem.* **2001**, *276*, 29275. (d) McEwen, D. P.; Gee, K. R.; Kang, H. C.; Neubig, R. N. *Anal. Biochem.* **2001**, *291*, 109. (e) Pace, H. C.; Hodawadekar, S. C.; Draganescu, A.; Huang, J.; Bieganowski, P.; Pekarsky, Y.; Brenner, C. *Curr. Biol.* **2000**, *10*, 907. (f) Draganescu, A.; Hodawadekar, S. C.; Gee, K. R.; Brenner, C. *J. Biol. Chem.* **2000**, *275*, 4555.

(45) Marcus, R. A. *Discuss. Faraday Soc.* **1960**, *29*, 21.

(46) (a) Benniston, A. C.; Harriman, A.; Grosshenny, V.; Ziessel, R. *New J. Chem.* **1997**, *21*, 405. (b) Grosshenny, V.; Harriman, A.; Ziessel, R. *Angew. Chem., Int. Ed.* **1995**, *34*, 1100.

(47) (a) Bixon, M.; Jortner, J. *Adv. Chem. Phys.* **1999**, *106*, 35. (b) Kroon, J.; Oevering, H.; Verhoeven, J. W.; Warman, J. M.; Oliver, A. M.; Paddon-Row, M. N. *J. Phys. Chem.* **1993**, *97*, 5065. (c) Smit, K. J.; Warman, J. M.; de Haas, M. P.; Paddon-Row, M. N.; Oliver, A. M. *Chem. Phys. Lett.* **1988**, *152*, 177. (d) Liang, N.; Miller, J. R.; Closs, G. L. *J. Am. Chem. Soc.* **1990**, *112*, 5353. (e) Warman, J. M.; Smit, K. J.; Jonker, S. A.; Verhoeven, J. W.; Oevering, H.; Kroon, J.; Paddon-Row, M. N.; Oliver, A. M. *Chem. Phys.* **1993**, *170*, 359.

(48) Okada, T.; Karaki, I.; Matsuzawa, E.; Mataga, N.; Sakata, Y.; Misumi, S. *J. Phys. Chem.* **1981**, *85*, 3957.

(49) Li, F.; Yang, S. I.; Ciringh, Y.; Seth, J.; Martin, C. H., III; Singh, D. L.; Kim, D.; Birge, R. R.; Bocian, D. F.; Holten, D.; Lindsey, J. S. *J. Am. Chem. Soc.* **1998**, *120*, 10001.

(50) Hattori, S.; Ohkubo, K.; Urano, Y.; Sunahara, H.; Nagano, T.; Wada, Y.; Tkachenko, H.; Lemmetyinen, H.; Fukuzumi, S. *J. Phys. Chem. B* **2005**, *109*, 15368.

(51) McGylnn, S. P.; Azumi, T.; Kinoshita, M. *Molecular Spectroscopy of the Triplet State*; Prentice-Hall: Englewood Cliffs, NJ, 1969.

(52) Numerous examples exist where bodipy dyes have been used as donors or acceptors in energy-transfer units. See for example: (a) Wan, C.-H.; Burghart, A.; Chen, J.; Bergstrom, F.; Johansson, B. B.-A.; Wolford, M. F.; Kim, T. G.; Topp, M. R.; Hochstrasser, R. M. Burgess, K. *Chem. Eur. J.* **2003**, *9*, 4430. (b) Keller, R. C.; Silvius, J. R.; De Kruijff, B. *Biochem. Biophys. Res. Commun.* **1995**, *207*, 508. (c) Isaksson, M.; Kalinin, S.; Lobov, S.; Wang, S.; Ny, T.; Johansson, L. B.-A. *Phys. Chem. Chem. Phys.* **2004**, *6*, 3001. (d) Johansson, B. B.-A.; Karolin, J. *Pure Appl. Chem.* **1997**, *69*, 760. (e) Holten, D.; Bocian, D. F.; Lindsey, J. S. *Acc. Chem. Res.* **2002**, *35*, 57.